



## DULLRAZOR®: A SOFTWARE APPROACH TO HAIR REMOVAL FROM IMAGES

TIM LEE<sup>1</sup>, VINCENT NG<sup>2</sup>, RICHARD GALLAGHER<sup>13</sup>, ANDREW COLDMAN<sup>1</sup> and DAVID MCLEAN<sup>3</sup>

<sup>1</sup> Cancer Control Research, British Columbia Cancer Agency, Vancouver, Canada

<sup>2</sup> Department of Computing, Hong Kong Polytechnic University, Hong Kong

<sup>3</sup> Divisions of Dermatology, Vancouver Hospital and Health Sciences Centre and the University of British Columbia, Vancouver, Canada

(Received 26 November 1996; revised 25 March 1997)

**Abstract**—Recently, there has been a growing number of studies applying image processing techniques to analyze melanocytic lesions for atypia and possible malignancy and for total-body mole mapping. However, such lesions can be partially obscured by body hairs. None of these studies has fully addressed the problem of human hairs occluding the imaged lesions. In our previous study we designed an automatic segmentation program to differentiate skin lesions from the normal healthy skin, and learned that the program performed well with most of the images, the exception being those with hairs, especially dark thick hairs, covering part of the lesions. These thick dark hairs confused the program, resulting in unsatisfactory segmentation results. In this paper, we present a method to remove hairs from an image using a pre-processing program we have called DullRazor®. This pre-processing step enables the segmentation program to achieve satisfactory results. DullRazor® can be downloaded as shareware from <http://www.derm.ubc.ca>. © 1997 Elsevier Science Ltd.

Hair removal      Skin imaging      Image processing      Grayscale morphology  
Adaptive median filter

### 1. INTRODUCTION

Since 1994, we have been conducting a clinical study to analyze melanocytic lesions using computer image processing techniques [1-3], with the goal of eventually developing a diagnostically useful machine based on recognition algorithms for atypical melanocytic lesions. A weekly imaging session was held in the Pigmented Lesion Clinic of the Division of Dermatology, the University of British Columbia and Vancouver Hospital to digitize nevi under a controlled environment. Patients were first screened by a dermatologist (DM). Any abnormal lesions were marked and the clinical symptoms, such as asymmetry, border irregularities, colour, and size, were scored. An RGB colour was obtained for each abnormal lesion using a hand-held video microscopy camera, with a 20 times magnification lens.

As the first step to analyze the images, we designed an automatic segmentation program to separate the lesions from the normal surrounding skin [2]. Colour images were first filtered by a multi-stage median filter to remove noise, but keep the structure and fine details. A threshold value was carefully chosen for each of the three different colour bands, and a simple rule-based system was used to merge the three colour bands to form the final segmentation. In the study, we found most images could be segmented successfully by the program. However, the images with hairs, specially thick dark hairs occluding part of the lesion, gave unsatisfactory results because these hairs confused the segmentation algorithm (see Figs 1 and 2). In this paper, we present an algorithm, called DullRazor®, that removes such dark hairs from the image.

The hair problem has not been fully addressed in the literature of computer image

\*Author to whom correspondence should be addressed at: Cancer Control Research, British Columbia Cancer Agency, 600 W 10th Ave., Vancouver, B.C., Canada V5Z 4E6.

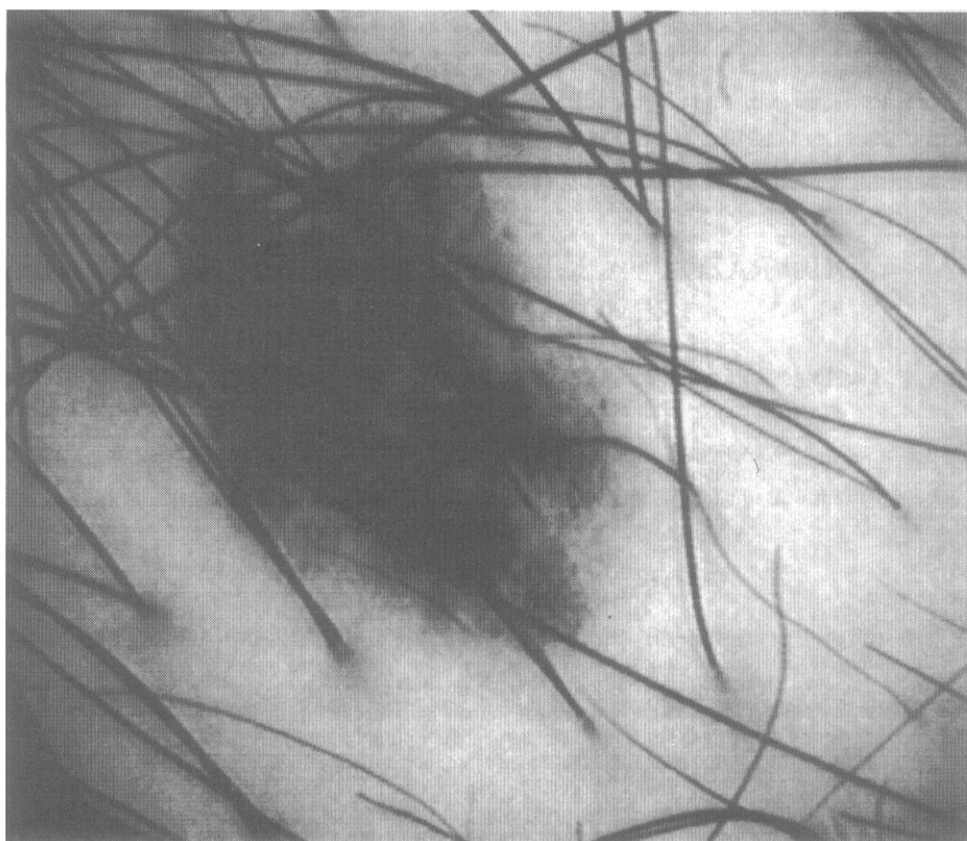


Fig. 1. A lesion occluded by dark thick hairs.

processing techniques for dermatological applications in spite of the rapid growth of this field [4–6]. It is an important issue, however, especially for designing automatic segmentation and feature extraction algorithms for clinical use. In a similar study conducted in Italy [7,8], the investigators decided to shave the hairs using a razor before the imaging session. This procedure not only adds extra costs and time to the imaging session, but also is impractical if we want to apply the technology to total-body nevus imaging [9,10]. In our opinion, a software approach is a more cost-effective and practical solution.

With the software approach, there are different ways to handle the hair problem. Since the image consists mostly of hairs, lesion, and healthy normal skin, one approach is to modify the segmentation program to recognize all these objects. This method, however, will complicate the segmentation program due to the hairs dividing a single lesion into many sub-parts. The enhanced segmentation program must be able to join all the sub-parts together to form a single lesion. This merging process is a nontrivial task. Instead of modifying the segmentation program, we took another approach—using DullRazor® as a pre-processor to remove thick and dark hairs. Then the segmentation algorithm can be kept simple. Our software technique can also probably be adapted for the documentation and assessment of other dermatological conditions.

## 2. METHODS

Our video microscopy imaging device is a hand-held camera connected to a shoebox-sized main unit, which is further connected to a frame grabber in a personal computer (PC). The main unit also houses the light source, a halogen bulb. Guided by optic fibers to the edge of the hand-held camera, the light source forms a ring within a hollow cylinder attached to the camera. The cylinder is in direct contact with the patient skin and it stabilizes the camera against excessive lateral or vertical movement, when an RGB image is digitized. Because the hand-held camera is both small and light in weight, it can be moved around the patient's skin surface easily to capture images of skin lesions on different body parts.

The RGB colour images are  $512 \times 486$  pixels in size, with spatial resolution

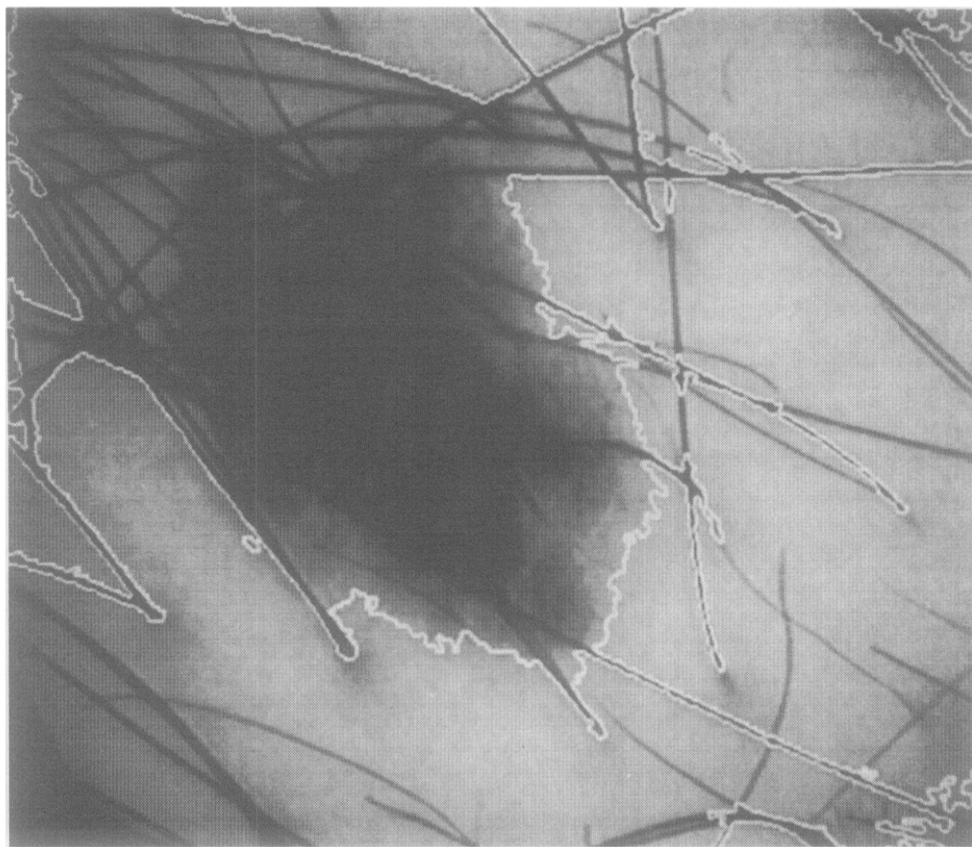


Fig. 2. Incorrect segmentation result of Fig. 1. because the hairs confused the automatic segmentation program. The white line outlines the lesion border detected by the automatic segmentation program.

0.033 mm × 0.025 mm. Each image has one or more lesions located near the centre and the lesions are surrounded by normal skin of differing hue. Some images also contain an additional image of the blue marker used by the physician (DM) to designate which lesion was to be imaged. The lesion can vary in size, shape, colour and saturation. In many cases, the margin between a lesion and the surrounding skin was clinically ill-defined.

For this DullRazor® algorithm, we are interested in removing only the thick dark hairs.

0 1 1 1 1 1 1 1 1 1 1 0	0 0 0 0 0 0 0 0 0	0
	0 1 0 0 0 0 0 0 0	1
	0 0 1 0 0 0 0 0 0	1
	0 0 0 1 0 0 0 0 0	1
	0 0 0 0 1 0 0 0 0	1
	0 0 0 0 0 1 0 0 0	1
	0 0 0 0 0 0 1 0 0	1
	0 0 0 0 0 0 0 1 0	1
	0 0 0 0 0 0 0 0 1	1
		1
		1
		1
		0
(a)	(b)	(c)

Fig. 3. Structure element for the generalized closing operation. (a) horizontal structure element, centered at (6, 0), (b) diagonal structure element, centered at (4, 4), (c) vertical structure element, centered at (0, 6).

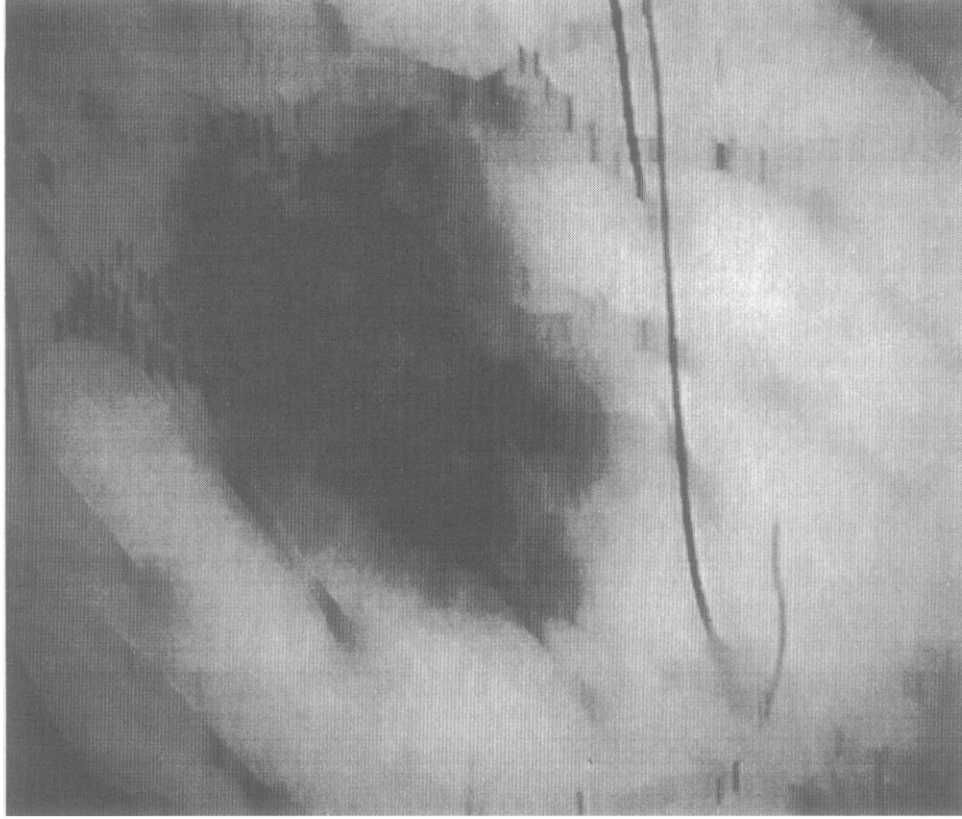


Fig. 4. One of the grayscale closing images. This image is obtained when the vertical structure, Fig. 3(c), is applied to Fig. 1.

The algorithm consists of three basic steps: (1) identifying the dark hair locations; (2) replacing the hair pixels by the nearby non-hair pixels; and (3) smoothing the final result.

(1) To locate the dark hairs, a generalized grayscale morphological closing operation is applied to the three colour bands separately [11]. The grayscale closing operation *smoothes* out the low intensity values, i.e. the thick dark hair pixels, along the structure element direction. Experimental results suggest that three structure elements at different directions, 0° (horizontal), 45° (diagonal), and 90° (vertical) as illustrated in Fig. 3, are adequate to *smooth* out all the black hairs. The generalized grayscale closing image is obtained by taking the maximum response of the grayscale closing results at all three specified directions. Finally, a binary hair mask image is created by thresholding the absolute difference between the original colour band and the generalized grayscale closing image. This hair mask divides the hair and non-hair regions into disjoined areas.

Let  $G_r$  be the generalized grayscale closing image of the original red band,  $O_r$ , and  $S_0$ ,  $S_{45}$ , and  $S_{90}$  are the structure elements in the horizontal, diagonal, and vertical direction.  $G_r$  can be expressed as

$$G_r = |O_r - \max\{O_r \bullet S_0, O_r \bullet S_{45}, O_r \bullet S_{90}\}|, \quad (1)$$

where  $\bullet$  denotes the grayscale closing operation. Furthermore, the binary hair mask pixel at the location  $(x,y)$ ,  $M_r(x,y)$ , is computed as

$$\begin{aligned} M_r(x,y) &= 1, & \text{if } G_r(x,y) > T \\ &= 0, & \text{otherwise} \end{aligned}, \quad (2)$$

where  $T$  is a pre-defined threshold value.

A similar expression can be written for the green and blue bands. The final hair mask for the original image,  $M$ , is the union of the hair masks for the three colour bands.

$$M = M_r \cup M_g \cup M_b, \quad (3)$$

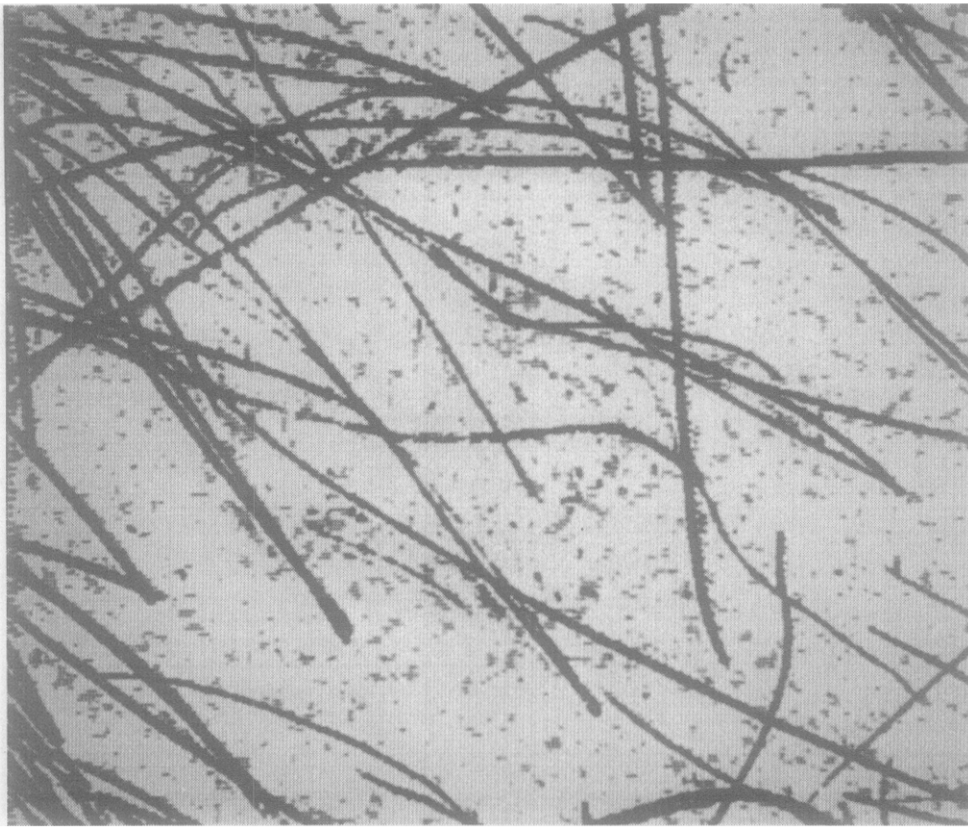


Fig. 5. Hair mask  $M$  of Fig. 1. The potential hair pixels are shown in black. These pixels are further verified to remove the noise pixels.

where  $M_r$ ,  $M_g$ , and  $M_b$  are the hair masks for the corresponding colour bands. Figure 4 illustrates the grayscale closing result of one of the structures applying to Figs 1 and 5 shows the corresponding hair mask  $M$ .

(2) In this interpolation step, the binary hair mask,  $M$ , obtained in step (1), is used to guide the replacement operation, replacing the corresponding pixel value in the original image by the nearby non-hair pixel values. Before the replacement operation is performed, each pixel in the hair region of the mask  $M$  is checked to ensure that it is located within a thin and long structure, i.e. the hair structure; otherwise, it is rejected as noise.

For each pixel inside the hair region of  $M$ , line segments are drawn in eight directions, up, down, left, right and the four diagonals, radiating from the pixel until the segment reaches the non-hair region. These eight line segments form four straight lines centering at the pixel. Lengths of the lines are calculated and the longest one is noted. The longest line must be longer than 50 pixels and other lines must be shorter than 10 pixels. Otherwise, the pixel is rejected.

When a pixel is verified to be inside the hair structure, its corresponding pixel in the original image is replaced, using bilinear interpolation, by two nearby non-hair pixel values along the shortest line, the line perpendicular to the longest one. Since the binary hair mask,  $M$ , is constructed by the thresholding method described in step (1), the exact hair border locations cannot be delineated due to the non-preciseness of the threshold value, image noise and the penumbra effect on the hairs (the nearby area of a hair is slightly darker due to the partial shadowing). To overcome the border problem, the non-hair pixels, 11 pixels away from the two sides of the hair borders and along the shortest line segment, are selected for the interpolation algorithm.

Let  $I(x,y)$  be the intensity value for the replacing pixel,  $I_1(x_1,y_1)$  and  $I_2(x_2,y_2)$  be the selected non-hair pixel intensities along the shortest direction. The new intensity value  $I_n(x,y)$  can be expressed as

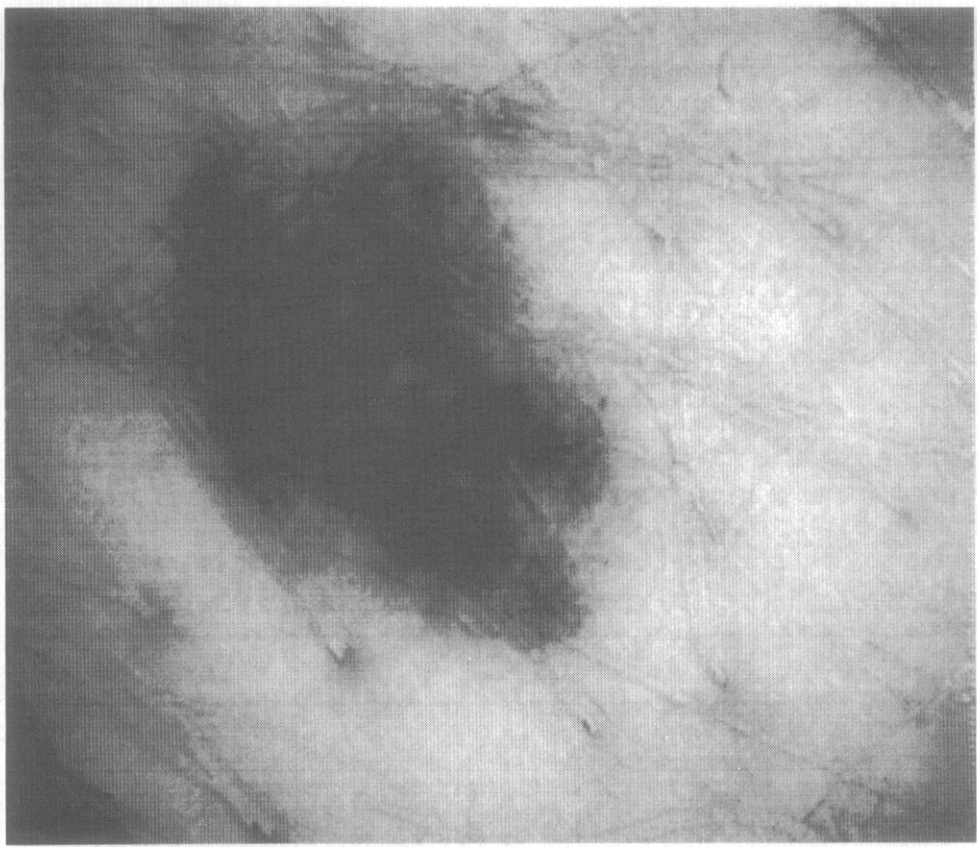


Fig. 6. The hair pixels are replaced by the nearby non-hair pixels. Thin lines near the hair border are caused by the non-preciseness of the replacement values.

$$I_n(x,y) = I_2(x_2,y_2) * \frac{D(I(x,y), I_1(x_1,y_1))}{D(I_1(x_1,y_1), I_2(x_2,y_2))} + I_1(x_1,y_1) * \frac{D(I(x,y), I_2(x_2,y_2))}{D(I_1(x_1,y_1), I_2(x_2,y_2))}, \quad (4)$$

where

$$D(A(a,b),B(c,d)) = \sqrt{(c-a)^2 + (d-b)^2}.$$

(3) As discussed in the previous step, the exact border locations are hard to identify due to the thresholding method, image noise and the penumbra effect. Thin lines are usually formed near the border of the hair regions (Fig. 6). In this step, an adaptive median operator is employed to smooth out these thin lines. Using a binary dilation operation with a  $5 \times 5$  square structure element of all 1's, centering at the middle of the square, a new hair mask with slightly enlarged hair regions is constructed. The new hair mask is shown in Fig. 7. An  $5 \times 5$  median filter is applied to the enlarged hair regions, while the non-hair regions are left untouched to preserve the fine details.

### 3. RESULTS AND DISCUSSION

The algorithm, DullRazor®, was implemented in C using a Sun SPARCstation 2. All constant values were empirically determined. The threshold value  $T$  in equation (1) was set to 24. Running DullRazor as the pre-processing step, our automatic segmentation program could produce satisfactory result even with the hairy images (Figs 2 and 8). Indeed there was often striking improvement with the image segmenting correctly, freed from most of the deleterious effects of hairs.

There are problems inherent to this software solution. Using the software method with a single view, the pixel values underneath the hairs, obviously, could not be reconstructed accurately. With careful examination, traces of faded hair lines were sometimes visible, which is why the program is called DullRazor®. These traces could probably be removed, but at the cost of an excessive loss of fine detail in the image. For the purpose of using

DullRazor® as a pre-processing step for an automatic segmentation program, these artifacts did not alter the final segmentation result. Depending upon the needs of later image manipulation and analysis, the replaced pixels could be excluded from further analysis using the same hair mask.

Rarer problems are replacement pixels darker than appropriate due to shadowing, and areas of very heavy hair overlap being uninterpretable by the algorithm. Figure 9 shows an image heavily covered by thick hairs. Without DullRazor® as the pre-processing step, our simple segmentation program was confused by the hairs and declared almost the entire image as a lesion. However, after the pre-processing step was applied, the accurate segmentation result was obtained (Fig. 10). Reconstructed areas corresponding to the hair clusters near the top of the lesion and on the right side of the image had an overly dark appearance because by blocking the lighting source, the hair cluster reduced the light to the nearby regions that were used as replacement values. However, the automatic segmentation program was still able to detect the lesion.

Figures 11 and 12 show an example where, although a much improved image was generated, a small region near the bottom of the image was misclassified as lesion due to the heavy hair cluster. Otherwise, the segmentation result was accurate.

In addition to clarifying images of pigmented lesions so as to permit segmentation analysis, modifications of this software program may have other applications in medicine. In dark haired individuals, the number of pixels should correlate broadly with the amount of hair in the original image. Sequential images of, for instance, a shaved patch of scalp should be assessable in a way that would generate an index of increase in hair mass. Both linear growth of the hair and increase in hair bulk (thickness) should influence the final change in the quantitation of hair mass. This could be of use in the assessment of therapeutic interventions in the treatment of alopecia. Presently accepted methodology involves the manual counting of hair, with the assessment of growth in hair mass, including

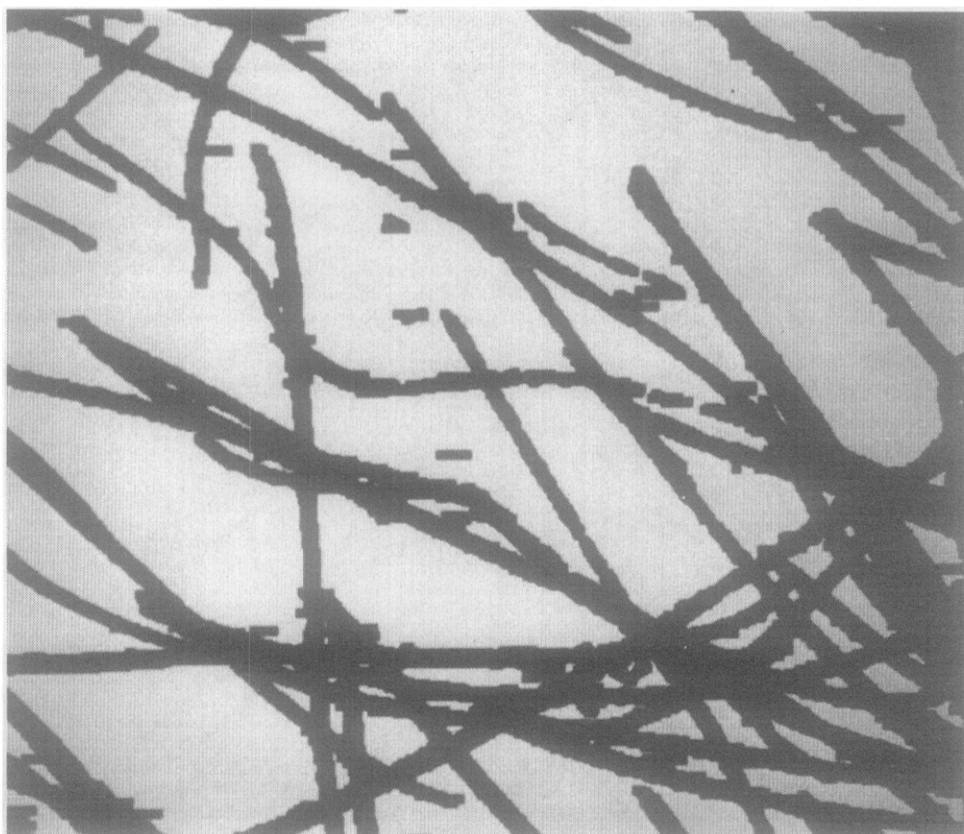


Fig. 7. The new hair mask with a slightly enlarged hair structure. After the hair mask  $M$  is verified so that noise pixels are removed, a binary dilation operation with a  $5 \times 5$  element structure of all 1's, centering at the middle of the square, is applied to obtain this new hair mask.

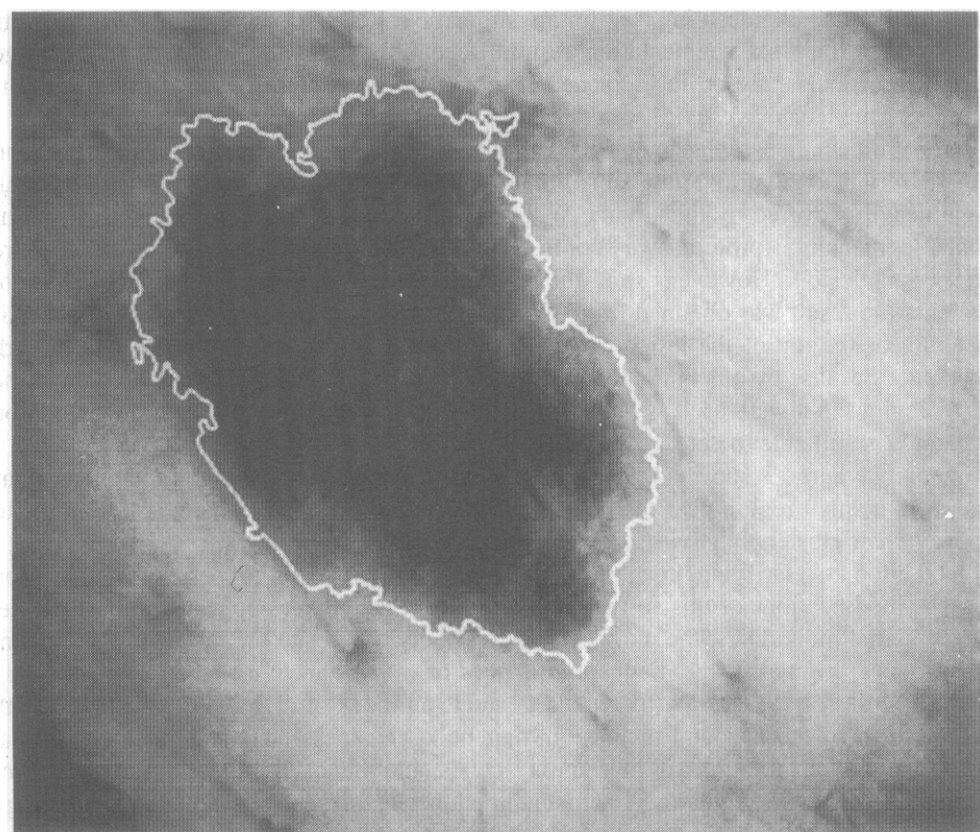


Fig. 8. New segmentation result with DullRazor® pre-processing step. The white line outlines the lesion border detected by the automatic segmentation program.

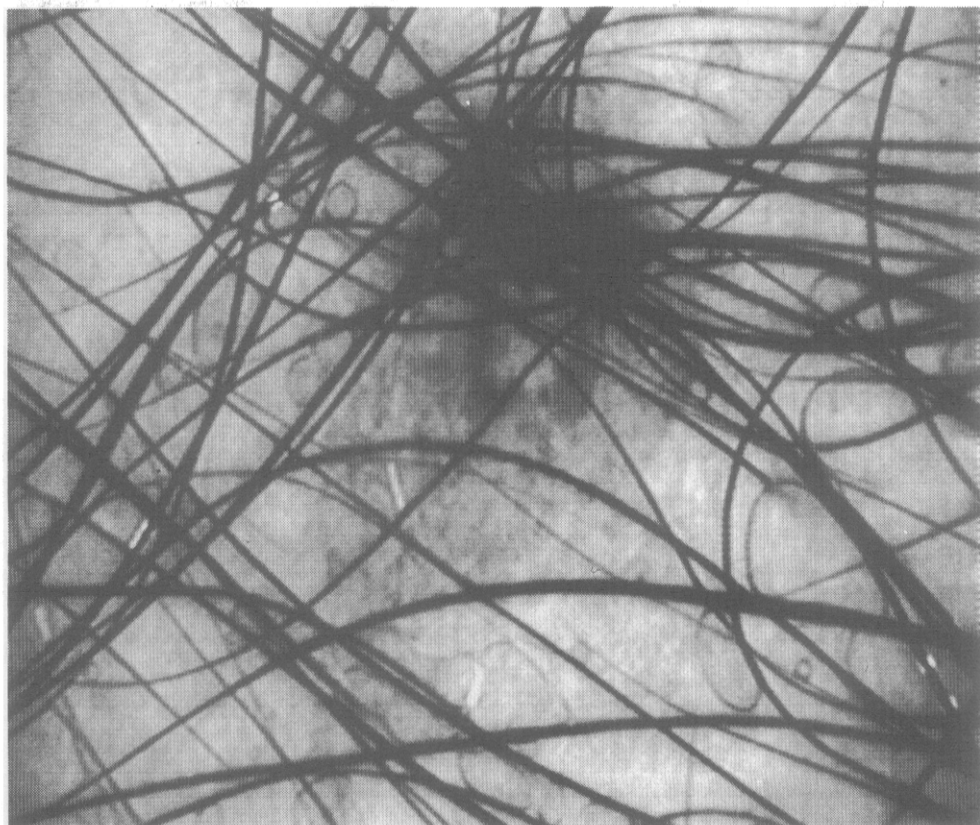


Fig. 9. A lesion heavily covered by dark thick hairs.

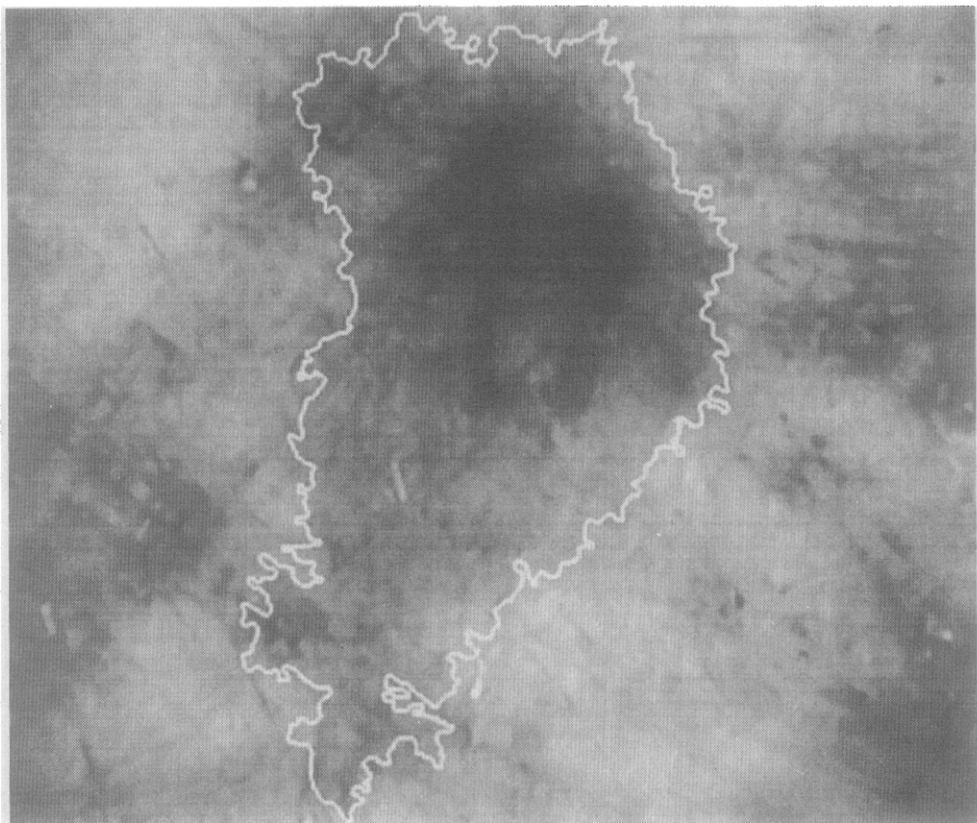


Fig. 10. Segmentation result of Fig. 9. The white line outlines the lesion border detected by the automatic segmentation program.

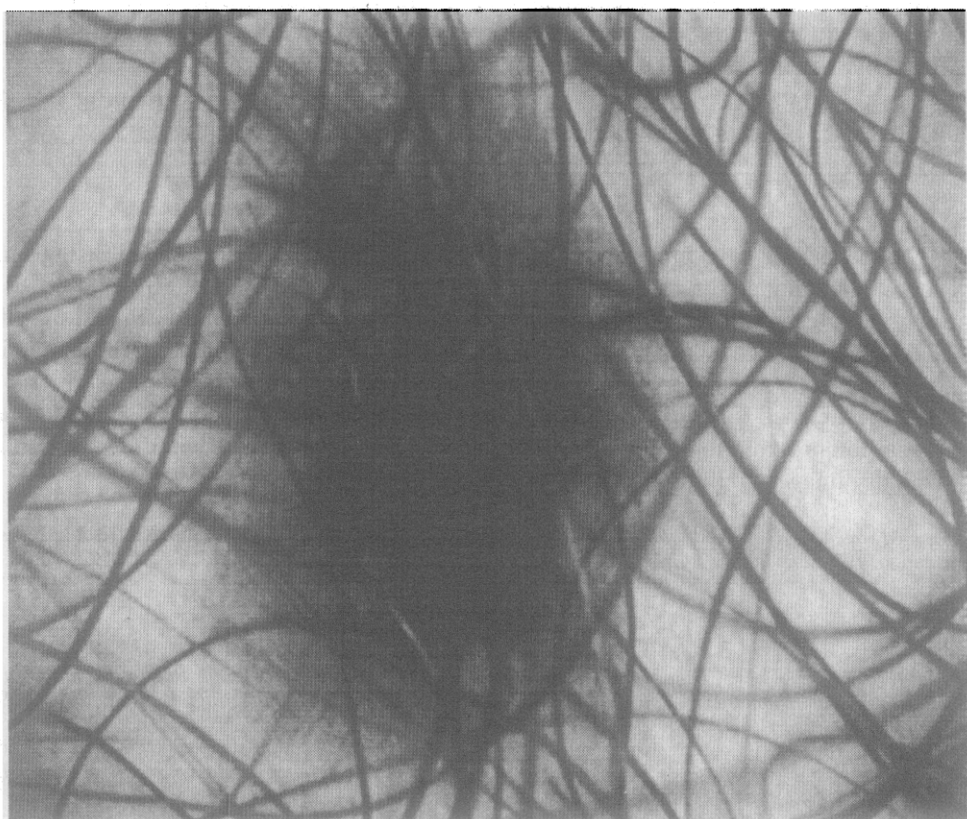


Fig. 11. Another lesion heavily covered by dark thick hairs.

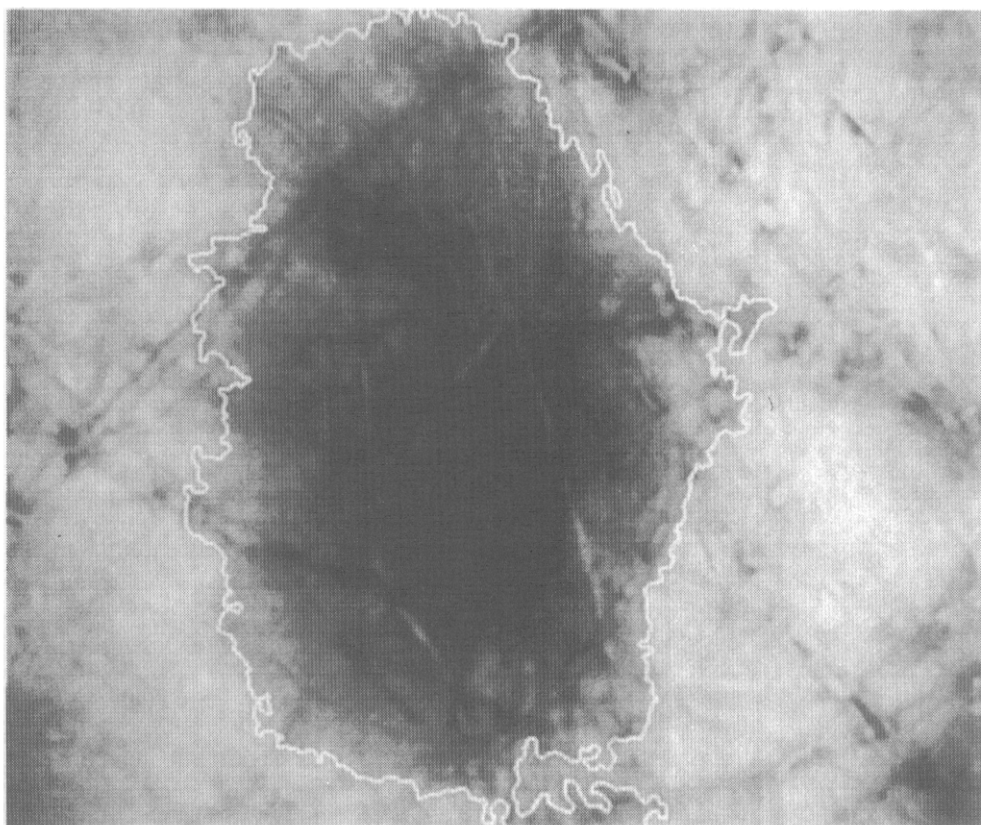


Fig. 12. Segmentation result of Fig. 11. The white line outlines the lesion border detected by the automatic segmentation program.

the assessment of growth rate and hair bulk being very problematic unless the scalp is shaved at each visit and the hair separated from shaved skin cells prior to weighing.

Similarly, such an approach might allow for the development of an index related to the vascularity of images of the retina. This could be useful in monitoring the progression of retinal disease, or the response of such disease to therapeutic intervention.

#### 4. CONCLUSION

In this paper, we have presented a step-by-step algorithm for hair removal using image processing technique. In our opinion, it is more practical and cost-effective to use a software approach to remove hairs, rather than mechanically shaving each lesion before images are captured. The improvement in our automatic segmentation program that defines lesion from non-lesion, separating lesions from the normal healthy skin, supports the potential relevance of this technique. This pre-processing step helps the automatic segmentation program to achieve a satisfactory result despite the hair interference. Without it, the hairy images could not have been used for any further analysis.

*Acknowledgements*—This work was supported in part by grants from British Columbia Health Research Foundation, 182(92-2) and 183(92-2).

#### REFERENCES

1. V. Ng and A. Coldman, Diagnosis of melanoma with fractal dimensions, *IEEE Region 10 International Conference on Computers, Communications, Control and Power Engineering*, Beijing, China, 19–21 October, 514–517 (1993).
2. T. Lee, V. Ng, D. McLean, A. Coldman, R. Gallagher and J. Sale, A multi-stage segmentation method for images of skin lesions, *Proceedings of IEEE Pacific Rim 1995 Conference on Communications, Computers, Visualization, and Signal Processing*, May, 602–605 (1995).
3. V. Ng and T. Lee, Measuring border irregularities of skin lesions using fractal dimensions, *SPIE Photonics China, Electronic Imaging and Multimedia Systems*, Volume 2898, Nov, 64–72 (1996).

4. R. White, D. Rigel and R. Friedman, Computer applications in the diagnosis and prognosis of malignant melanoma, *Dermatol. Clin.*, **9**, 695–702 (1991).
5. W.V. Stoecker, R. Moss, F. Ercal and S. Umbaugh, Nondermatoscopic digital imaging of pigmented lesions, *Skin Res. Technol.*, **1**, 7–16 (1995).
6. P.N. Hall, E. Claridge and J.D. Morris Smith, Computer screening for early detection of melanoma—is there a future?, *Br. J. Dermatol.*, **132**, 325–338 (1995).
7. L. Andreassi, R. Perotti, M. Burroni, G. Dell'eva and M. Biagioli, Computerized image analysis of pigmented lesions, *Chronica Dermatol.*, **1**, 11–24 (1995).
8. S. Seidenari, M. Burroni, G. Dell'eva, P. Pepe and B. Belletti, Computerized evaluation of pigmented skin lesion images recorded by a videomicroscope: comparison between polarizing mode observation and oil/slide mode observation, *Skin Res. Technol.*, **1**, 187–191 (1995).
9. W. Slue, A.W. Kopf and J.K. Rivers, Total body photographs of dysplastic nevi, *Arch. Dermatol.*, **124**, 1239–1243 (1988).
10. H. Voigt and R. Claßen, Topodermatographic image analysis for melanoma screening and the quantitative assessment of tumor dimension parameters of the skin, *Cancer*, **75**, 981–988 (1995).
11. R. Haralick and L. Shapiro, *Computer and Robot Vision*, Vol. 1. Addison-Wesley, Reading, MA (1992).

**About the Author**—TIM LEE is currently working at Cancer Control Research, British Columbia Cancer Agency. His research interests include medical imaging, computer vision, and networking.

He received his BSc in Mathematics and Computer Science and MSc in Computer Science from the University of British Columbia in 1980 and 1983, respectively.

**About the Author**—VINCENT NG received the BSc degree in mathematics and computing science from the Simon Fraser University, Canada in 1982. He later studied in the University of Waterloo, Canada, and received his M. Math degree there in 1986. In 1994, he received his PhD degree from Simon Fraser University.

Since 1994, he has been an assistant professor in the Hong Kong Polytechnic University. His research interests include spatial databases, data mining, medical informatics and medical imaging.

**About the Author**—RICHARD GALLAGHER graduated from the University of British Columbia (UBC) in 1967 with a degree in Biological Sciences. In 1973, he received his masters in Medical Sociology from the University of Western Washington and is also a Fellow of the American College of Epidemiology.

At present, he is A/Leader, Cancer Control Research Unit at the British Columbia Cancer Agency; Clinical Associate Professor, Department of Health Care and Epidemiology, Faculty of Medicine, UBC; and an Associate Member, Division of Dermatology, Faculty of Medicine at UBC. His research focus is in three topic areas in the epidemiology of cancer: melanoma and non-melanocytic skin cancer, prostate cancer and occupational cancer.

**About the Author**—ANDREW COLDMAN is currently the head of a group concerned with the population health and evaluation of cancer related outcomes in the British Columbia Cancer Agency. He also holds adjunct appointments in the Departments of Statistics and Health Care and Epidemiology at the University of British Columbia. He has degrees in statistics and epidemiology and his research interests relate to the determinants of outcome. His main research work has been done in the area of the development of drug resistance to anti-neoplastic agents.

**About the Author**—DAVID MCLEAN received his BSc (Med) and MD in 1971 from the University of Manitoba, and FRCPC, Dermatology in 1976.

Currently, he is Professor and Head of Division of Dermatology, Faculty of Medicine at the University of British Columbia; and Head of Division of Dermatology of Vancouver Hospital and Health Sciences Centre. His research activities include autofluorescence properties of skin with potential applications in skin cancer detection and solar ultraviolet radiation effect on melanoma.